Sarco(endo)plasmic reticulum ATPase is a molecular partner of Wolfram syndrome 1 protein, which negatively regulates its expression

Zatyka, Malgorzata; Da Silva Xavier, G; Bellomo, Elisa A; Leadbeater, Wendy; Astuti, Dewi; Smith, Joel; Michelangeli, Francesco; Rutter, Guy A; Barrett, Timothy

DOI:
10.1093/hmg/ddu499
10.1093/hmg/ddu499

Document Version
Peer reviewed version

Citation for published version (Harvard):
Zatyka, M, Da Silva Xavier, G, Bellomo, EA, Leadbeater, W, Astuti, D, Smith, J, Michelangeli, F, Rutter, GA & Barrett, T 2015, 'Sarco(endo)plasmic reticulum ATPase is a molecular partner of Wolfram syndrome 1 protein, which negatively regulates its expression', *Human Molecular Genetics*, vol. 24, no. 3, pp. 814-827. https://doi.org/10.1093/hmg/ddu499, https://doi.org/10.1093/hmg/ddu499

Journal:	HMG..J
Article id:	DDU499

Colour on-line figure	none
Colour print figures	none

The following queries have arisen while collating the corrections. Please check and advise us on the below queries.

1.	As per author correction Figure 8 has been converted into black and white. Kindly check.	

Human Molecular Genetics, 2014, Vol. 23, No. ? **1–14**
doi:10.1093/hmg/ddu499
Advance Access published on September 30, 2014

Sarco(endo)plasmic reticulum ATPase is a molecular partner of Wolfram syndrome 1 protein, which negatively regulates its expression

Malgorzata Zatyka[1], Gabriela Da Silva Xavier[5], Elisa A. Bellomo[5], Wendy Leadbeater[2], Dewi Astuti[1], Joel Smith[1], Frank Michelangeli[3,4], Guy A. Rutter[5] and Timothy G. Barrett[1,*]

[1]Department of Medical and Molecular Genetics, [2]Department of Neurotrauma and Neurodegeneration, [3]School of Clinical and Experimental Medicine, The Medical School, [4]School of Biosciences, University of Birmingham, Birmingham B15 2TT, UK and [5]Department of Cell Biology, Division of Medicine, Faculty of Medicine, Imperial Centre for Translation and Experimental Medicine, Hammersmith Hospital, Du Cane Road, London W12 0NN, UK

Received June 24, 2014; Revised September 21, 2014; Accepted September 26, 2014

Wolfram syndrome is an autosomal recessive disorder characterized by neurodegeneration and diabetes mellitus. The gene responsible for the syndrome (*WFS1*) encodes an endoplasmic reticulum (ER)-resident transmembrane protein that is involved in the regulation of the unfolded protein response (UPR), intracellular ion homeostasis, cyclic adenosine monophosphate production and regulation of insulin biosynthesis and secretion. In this study, single cell Ca^{2+} imaging with fura-2 and direct measurements of free cytosolic ATP concentration ($[ATP]_{CYT}$) with adenovirally expressed luciferase confirmed a reduced and delayed rise in cytosolic free Ca^{2+} concentration ($[Ca^{2+}]_{CYT}$), and additionally, diminished $[ATP]_{CYT}$ rises in response to elevated glucose concentrations in WFS1-depleted MIN6 cells. We also observed that sarco(endo)plasmic reticulum ATPase (SERCA) expression was elevated in several WFS1-depleted cell models and primary islets. We demonstrated a novel interaction between WFS1 and SERCA by co-immunoprecipitation in Cos7 cells and with endogenous proteins in human neuroblastoma cells. This interaction was reduced when cells were treated with the ER stress inducer dithiothreitol. Treatment of WFS1-depleted neuroblastoma cells with the proteasome inhibitor MG132 resulted in reduced accumulation of SERCA levels compared with wild-type cells. Together these results reveal a role for WFS1 in the negative regulation of SERCA and provide further insights into the function of WFS1 in calcium homeostasis.

INTRODUCTION

There is increasing evidence that endoplasmic reticulum (ER) perturbation plays a critical role in cell death in both neurodegenerative disorders (1,2) and diabetes mellitus (3,4). Abnormal release of calcium from the ER has been observed in several pathological conditions affecting the nervous system (5,6). ER stress, oxidative stress, palmitate and chronic high glucose all decrease pancreatic beta-cell ER calcium levels, leading to beta-cell death (7).

The ER functions as a calcium store through the expression of at least three types of proteins: the sarco-endoplasmic reticulum calcium ATPase (SERCA) family of proteins that actively pump calcium into the ER; luminal calcium binding proteins for storing calcium and the gated calcium channels inositol trisphosphate receptors (IP3R) and ryanodine receptors (RyR) for the controlled release of calcium from the ER along its electrochemical gradient (8). ER calcium depletion may be associated with, among others, toxin interaction with the IP3R (GM1 gangliosidosis (9)); over-activation of the RyR (Gaucher disease (6)); SERCA inhibition (Sandhoff disease (10)) and increased SERCA expression as a compensatory mechanism through regulation by ATF6 during the ER stress response (11).

Childhood-onset diabetes mellitus and progressive optic atrophy are the diagnostic features of Wolfram syndrome, a genetic form of both diabetes and neurodegeneration (12). In this disease, pancreatic beta-cells and presumably neuronal cells are selectively destroyed due to mutations in the *WFS1*

*To whom correspondence should be addressed at: School of Clinical and Experimental Medicine, The Medical School, University of Birmingham, Birmingham B15 2TT, UK. Tel: +44-1-213339267; Fax: +44-1-213339272; Email: t.g.barrett@bham.ac.uk

gene, which encodes WFS1 protein or Wolframin, an ER transmembrane protein (13). The mechanism is thought to be through perturbed ER homeostasis (14,15) leading to ER stress (16,17). Loss of function mutations in *WFS1* has been shown to lead to ER calcium depletion (18), increased cytosolic calcium concentrations and increased expression of a pro-apoptotic molecule CHOP, leading to cell death (7). Reconstitution of this ER-resident transmembrane protein into planar lipid bilayers induced a cation-selective ion channel (19).

We have previously shown that Wolframin interacts with the ion pumps Na^+K^+ATPase and vacuolar-type H^+ATPase, (20,21) supporting its role in protein folding/maturation and insulin biosynthesis and secretion. In this study, while investigating the glucose signalling pathway in WFS1-depleted MIN6 cells, we observed increased SERCA protein expression. These observations prompted us to investigate the possibility of an interaction between WFS1 protein and SERCA.

RESULTS

Wolframin-depleted beta-cell lines show reduced insulin secretion in response to elevated glucose or KCl concentrations

Wolframin has been implicated in the normal control of stimulus-secretion coupling during regulated insulin secretion *in vivo* and *in vitro* (16,17). To study the effects of Wolframin depletion on insulin secretion and Ca^{2+} signalling in beta-cells, we used the MIN6 insulinoma cell line. These stable cell lines have been engineered to provide reduced *WFS1* expression using RNA interference, with 0% (wild-type), 50% [knockdown A (KDA)] or 70% [knockdown B (KDB)] reduction in Wolframin expression achieved by expression of suitable scrambled or anti-*WFS1* shRNAs (16,20).

Insulin release in response to glucose (30 versus 3 mmol/l) was decreased in *WFS1*-depleted cells (Fig. 1A). At 30 mmol/l glucose (30G), the percentage of insulin released was decreased 7-fold for KDA ($P = 2.2 \times 10^{-7}$) and 4-fold for KDB ($P = 4.5 \times 10^{-7}$) cells, respectively, in comparison to wild-type. At 3 mmol/l glucose (3G), and after depolarization with 50 mmol/l KCl (HK), the percentage of insulin released was also decreased in KDA and KDB cells, but only reached significance in the KDA cells.

Wolframin-depleted primary islets from *WFS1* conditional knockout mice show defective insulin secretion in response to glucose

To confirm that Wolframin is necessary for normal insulin secretion in response to high glucose we isolated pancreatic islets from beta-cell selective conditional *WFS1* knockout (KO) mice, a kind gift from Professor A Permutt (16). The mice were 10–13 week old males: either *WFS1* conditional KO mice ($Wfs1^{flox/flox}$ $Cre^{cre/+}$) *or Wfs1* positive 'floxed' littermates ($Wfs1^{flox/flox}$). We measured reduced Wolframin expression in protein lysates prepared from the islets by immunoblotting; beta actin (BA) was used as a loading control. The Wolframin expression was decreased by 70% in the KO islets in comparison to the controls (Fig. 1B). The residual Wolframin level probably reflected the presence of WFS1 protein-positive cells in these islets: all islet non-beta-cells were WFS1 protein positive; *cre* recombinase was expressed from the rat insulin 2 promoter (16).

The isolation of islets and insulin secretion assay were performed as described in 'Materials and Methods'. The percentage of insulin released in response to glucose (17 versus 3 mmol/l) during static incubation for 1 h was decreased about 65% in islets from *Wfs1* KO mice in comparison to size matched control islets: percentage of insulin released by control islets (C) = 1.55 ± 0.08%, while by KO islets = 0.54 ± 0.15%, $P = 0.0006$ (Fig. 1B). After depolarization with 20 mmol/l KCl (HK), the percentage of insulin released from KO islets was also reduced in comparison to the control but did not reach statistical significance. These results confirmed the results obtained in MIN6 cells and are consistent with previous *in vivo and* the *in vitro* findings (16,17,22).

Wolframin depletion results in a delayed and reduced glucose-induced rise in cytosolic free Ca^{2+}

The above results suggested that alterations in glucose sensing may result in diminished glucose-induced insulin secretion in *WFS1*-depleted cells. To explore this possibility further, we investigated glucose- and KCl-induced cytosolic calcium ($[Ca^{2+}]_i$) rises in single, fura-2-loaded cells. The baseline $[Ca^{2+}]_i$ for each cell type was calculated as the average of the first 180 s of each experiment in perifusion buffer containing 3 mmol/l glucose, using the ratio of the emissions after exciting the dye at 340 and 380 nm. There were no apparent differences in baseline $[Ca^{2+}]_i$ between the cell lines [340:380 ratios (F/F_0): wild-type cell 0.30 ± 0.005; KDA 0.28 ± 0.003; KDB 0.32 ± 0.004 and the F/F_0 at the start of experiment was assumed to be equal for each cell line].

In contrast, a delayed and reduced $[Ca^{2+}]_i$ rise was observed in response to an increase in glucose concentration from 3 to 30 mmol/l in *WFS1*-depleted MIN6 cells in comparison to wild-type cells; representative traces for wild-type, KDA and KDB cells are shown in Figure 2A–C. Quantitated by measurement of the area under the curve (AUC) following stimulation (Fig. 2D), the response in *WFS1*-depleted cells was reduced 2.2- to 2.4-fold in comparison to wild-type cells (AUC for wild-type, KDA and KDB were: 477.4 ± 21.6; 211.4 ± 21.6 and 199.1 ± 23.6, respectively; *P* values: wild-type versus KDA: $P = 3.2 \times 10^{-14}$; wild-type versus KDB: $P = 2.8 \times 10^{-12}$; KDA versus KDB: $P = 0.3$; wild-type $n = 61$, KDA $n = 36$, KDB $n = 21$ cells).

The delay before a detectable increase in $[Ca^{2+}]_i$ following stimulation with 30 mmol/l glucose was also more than 2-fold longer in *WFS1*-depleted cells than in wild-type cells (Fig. 2E). While the wild-type cells responded after 203.7 ± 6.8 s, KDA and KDB cells responded only after 410.0 ± 12.9 and 416.7 ± 15.4 s, respectively (*P* values: wild-type versus KDA: $P = 6.2 \times 10^{-18}$; wild-type versus KDB: $P = 7.3 \times 10^{-16}$; KDA v KDB: $P = 0.3$). All cell lines responded similarly to depolarization with 50 mmol/l KCl (Fig. 2A–C). The response to 50 mmol/l KCl was quantitated by measurement of the AUC and is presented on Figure 2F (AUC for wild-type, KDA and KDB were: 435.1 ± 9.0; 447.3 ± 15.8, and 445.1 ± 16.2, respectively, wild-type $n = 61$, KDA $n = 36$, KDB $n = 21$ cells).

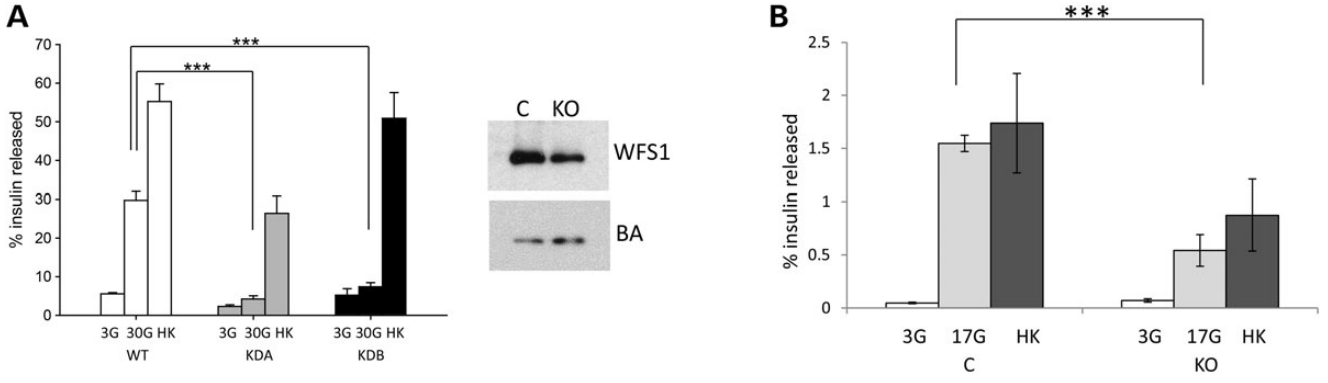

Figure 1. Glucose and depolarization-induced insulin secretion from MIN6 cells and isolated pancreatic islets. (**A**) Insulin secretion from wild-type and WFS1-depleted MIN6 cells. Quantitative analysis of insulin secreted in response to 30 mmol/l glucose and 50 mmol/l KCl. Total and released insulin were measured by radioimmunoassay as given under 'Materials and Methods'. Wolframin depletion resulted in a reduction of the percentage of insulin released in response to 30 mmol/l glucose (***wt versus KDA, $P = 2.2 \times 10^{-7}$, and wt versus KDB, $P = 4.5 \times 10^{-7}$). The results were from three experiments performed in triplicate. 3G: 3 mmol/l glucose, 30G: 30 mmol/l glucose, HK (high potassium): 50 mmol/l KCl. (**B**) Glucose-induced insulin secretion from primary islets isolated from conditional, beta-cell selective *Wfs1* KO mice. Immunoblot—70% reduced WFS1 expression in islets isolated from *Wfs1* KO mice in comparison to the control islets; 10 μg of protein extract was loaded per lane. BA: beta actin. Bar chart: quantitative analysis of insulin secreted in response to 17 mmol/l glucose and 20 mmol/l KCl measured by radioimmunoassay. The percentage of insulin released in response to 17 mmol/l glucose is significantly reduced in islets from KO mice in comparison to size matched control islets (C): (***C versus KO, $P = 0.0006$). The percentage of insulin released in response to high potassium (20 mmol/l) is also reduced in islets from KO mice, but it did not reach statistical significance (C versus KO, $P = 0.22$). No difference was measured in response to 3 mmol/l glucose (C versus KO, $P = 0.21$). The results come from at least three experiments in duplicates (for control islets (C), $N = 3$; for KO islets, $N = 6$). 3G: 3 mmol/l glucose, 17G: 17 mmol/l glucose, HK (high potassium): 20 mmol/l KCl.

Cytosolic free Ca^{2+} concentrations at baseline are not significantly different in Wolframin-depleted cells compared with wild-type cells

To confirm that there was no apparent differences in baseline $[Ca^{2+}]_i$ between the cell lines, we measured $[Ca^{2+}]_{CYT}$ in wild-type and KDB cells with cytosolic (untargeted) aequorin. Our results (Fig. 3) showed only a slightly higher level of cytosolic Ca^{2+} in KDB than in wild-type cells. The results come from two independent experiments (wild-type $n = 8$; KDB $n = 9$ separate measurements) and are consistent with our earlier findings of no significant differences in baseline $[Ca^{2+}]_i$ between the cell lines in single, fura-2-loaded cells.

Wolframin depletion results in a failure of glucose-induced rises in cytosolic free ATP concentrations

To investigate the causes of the reduced and delayed cytosolic $[Ca^{2+}]$ responses to high glucose, direct measurements of free cytosolic ATP concentration were performed by expressing recombinant firefly luciferase using an adenoviral vector (23,24), and using photon-counting (25). Luciferase catalyses the formation of oxyluciferin from luciferin and ATP. The production of light, with intensity proportional to the free concentration of ATP, can be detected with a suitably sensitive photon-counting device (26). Representative traces showing the apparent increase in free $[ATP]_{CYT}$ (as photon counts) for wild-type, KDA and KDB, respectively, are presented in Figure 4A–C, with quantitative analysis in Figure 4D. The increase in $[ATP]_{CYT}$ in response to high glucose was 14.1% ± 0.6 for the wild-type MIN6 cells (Fig. 4A), consistent with previous results (23,24,27) but only 4% ± 1.4 for KDA ($P = 7.43 \times 10^{-5}$) (Fig. 4B) and 1.3% ± 0.3 for KDB ($P = 1.8 \times 10^{-13}$) (Fig. 4C). The apparent rise in $[ATP]_{CYT}$ in response to high glucose was approximately 3-fold less in KDA than in wild-type MIN6 cells and about 10-fold lower in KDB than in wild-type MIN6 cells; (n, wt = 12, n, KDA = 6 and n, KDB = 12 runs in three separate experiments for KDB and two separate experiments for KDA) (Fig. 4D).

To determine whether changes in the apparent $[ATP]_{CYT}$ increase in response to glucose may be due to alterations in Ca^{2+} pumping into the ER or other intracellular stores, we monitored the impact of pharmacological depletion of these stores on the observed changes (Fig. 4). Interestingly, and in contrast to previous studies (28), inhibition of SERCA pumps with cyclopiazonic acid (CPA) decreased the magnitude of the glucose-induced rise in $[ATP]_{CYT}$ in wild-type cells, presumably reflecting enhanced ATP consumption for Ca^{2+} transport by other mechanisms [e.g. extrusion across the plasma membrane by plasma membrane Ca^{2+} ATPase (PMCA) or transporting into the lumen of Golgi with SPCA (secretory pathway Ca^{2+} ATPase) (Fig. 4A)]. In contrast, in both *WFS1*-depleted cell lines, SERCA inhibition increased free $[ATP]_{CYT}$ (Fig. 4B and C).

To confirm the above results we investigated ATP:ADP ratio rise to glucose using a different (static) method as described in 'Materials and Methods'. Briefly, cells were grown in six-well plates, starved overnight in medium with low glucose and on the day of the experiment incubated in buffers with either low glucose (3G), high glucose (30G) or high glucose and CPA (inhibitor of SERCA pump) and harvested in ice-cold perchloric acid (PCA). Determination of ATP levels was performed as previously described (29) and as given under 'Materials and Methods', the ATP:ADP ratio was calculated for all conditions. Our results show that ATP:ADP ratio rise to glucose is significantly smaller for KDB than for the control MIN6 cells: ATP:ADP ratio rise to glucose (30G versus 3G) was 1.24 ± 0.06, 1.06 ± 0.03 and 1.28 ± 0.06 for the control, KDB and KDA, respectively; only for KDB the difference reached the

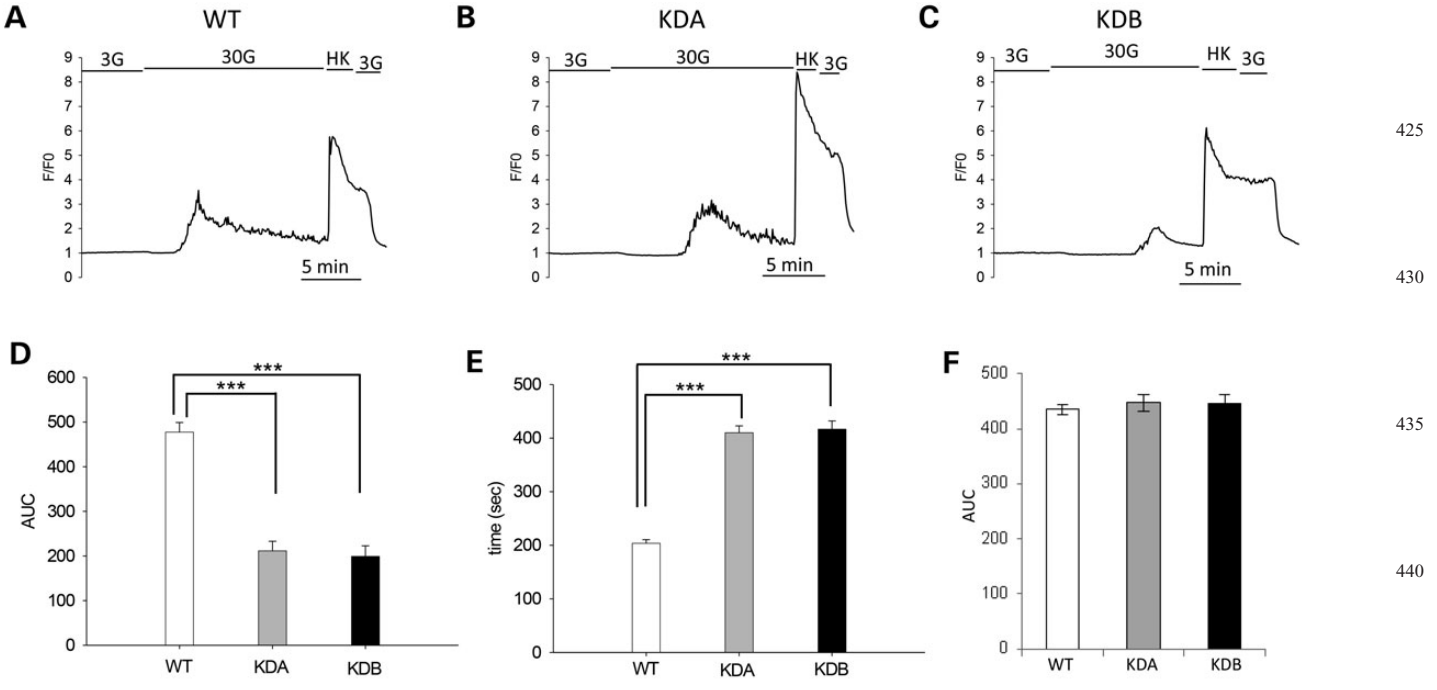

Figure 2. Changes in cytoplasmic free Ca^{2+} concentration in response to 30 versus 3.0 mmol/l glucose, or 50 mmol/l KCl in wild-type and Wolframin-depleted MIN6 cells. Representative traces of cytosolic free Ca^{2+}concentration changes in response to 30 (versus 3) mmol/l glucose for (**A**) *wt* MIN6; (**B**) KDA and (**C**) KDB cells. The *y* axes (F/F_0) represent the apparent free cytosolic [Ca^{2+}] as given by the normalized fluorescence intensity ratio of fura-2 upon excitation at 340 and 380 nm. Note the delayed and reduced rise in $[Ca^{2+}]_{CYT}$ in response to 30 mmol/l glucose in WFS1-depleted cells. 3G: 3 mmol/l glucose, 30G: 30 mmol/l glucose, HK (high potassium): 50 mmol/l KCl. (**D**) Quantitative analysis of the increase in free cytosolic Ca^{2+} concentration (fura-2) to 30 mmol/l glucose measured as AUC (area under curve). The response in WFS1-depleted cells was more than 2-fold smaller than *wt* (***wild-type versus KDA: $P = 3.2 \times 10^{-14}$, wild-type versus KDB: $P = 2.8 \times 10^{-12}$, and KDA versus KDB: $P = 0.3$). (**E**) Delayed response of cytosolic calcium rise to 30 mmol/l glucose in Wolframin-depleted cells. The delay before a detectable response was more than 2.0-fold longer in WFS1-depleted cells than in wild-type cells. (***wild-type versus KDA: $P = 6.2 \times 10^{-18}$; wild-type versus KDB: $P = 7.3 \times 10^{-16}$ and KDA versus KDB: $P = 0.3$). (**F**) Quantitative analysis of the increase in free cytosolic calcium concentration (fura-2) to 50 mmol/l KCl measured as AUC; there were no differences between WFS1-depleted cells and WT MIN6. *n*, wild-type = 61; *n*, KDA = 36; *n*, KDB = 21 cells.

statistical significance (*T* test CTRL versus KDB $P = 0.01$, CTRL versus KDA $P = 0.3$). These results confirmed our earlier finding that the ATP rise in response to high glucose is impaired in WFS1-depleted MIN6 cells.

Total ATP levels are reduced in WFS1-depleted cells

We next measured total ATP content in wild-type and *WFS1*-depleted MIN6 cells as described in 'Materials and Methods'. The results were normalized for the cell number and presented as relative luminescence units (RLU, proportional to the amount of ATP) per 10^4 cells (Table 1). The total levels of ATP (RLU) were significantly reduced in both WFS1-depleted cell lines to 79% (of the wild-type) in KDA and 53% in KDB.

SERCA expression is increased in WFS1-depleted cells

The decreased levels of cytosolic ATP could have been the result of an ATP generation defect or ATP overconsumption in WFS1-depleted cells. As no defect in oxidative phosphorylation was identified previously in Wolfram patient biopsies (30), there was a possibility that ATP may be over-consumed in WFS1-depleted cells. One of the major ATP consumers in pancreatic cells is the SERCA calcium pump. We hypothesized that SERCA over-activity could result in ATP depletion in WFS1-depleted cells and investigated the levels of SERCA expression.

We examined SERCA expression levels in several WFS1-depleted cell models: MIN6 pancreatic cells, primary pancreatic islets isolated from conditional *Wfs1* KO mice and in WFS1-depleted SK-N-AS neuroblastoma cells (Fig. 5). All the WFS1-depleted models displayed UPR activity, measured as an increase in the levels of ER stress markers (16,21).

To examine SERCA expression in MIN6 cells, we prepared extracts from microsomal fractions from control and WFS1-depleted KDA and KDB cell lines (32) and examined the levels of SERCA expression by immunoblotting using PanSERCA antibody Y1F4 (31). Protein disulfide isomerase (PDI) was used for normalization. In both WFS1-depleted cells KDA and KDB, the SERCA expression was increased over 2-fold in comparison to WFS1 positive control (KDA = 287.1 $\pm$ 82.2, $P = 0.045$, and KDB = 282.1 $\pm$ 83.0, $P = 0.052$, $n = 6$ for both, C = 100%, Fig. 5A).

To examine the SERCA expression levels in isolated islets, we prepared total protein extracts from 10 and 13 weeks old *Wfs1* conditional KO males as described in 'Materials and Methods'. There was a greater than 50% increase of SERCA levels in *Wfs1* conditional KO islets in comparison to *Wfs1* positive controls: (C = 100%, KO = 157.8 $\pm$ 17.8, $P = 0.005$, $n = 4$, Fig. 5B). Wolfram syndrome manifests also as a neurodegenerative disease. Therefore, we used three WFS1-depleted

neuroblastoma cell lines (KD1–KD3) depleted by 60–80% in comparison to the control (C) as described by Gharanei *et al*. (21) and examined the SERCA expression using either PanSERCA antibody Y1F4 (Fig. 5C) or isoform SERCA2-specific antibody (Fig. 5D). The expression levels of SERCA were increased in all WFS1-depleted cell lines. Figure 5C shows the increased expression levels detected with PanSERCA antibody (KD1 = 261.8% ± 30.8, $P = 0.02$, $n = 3$; KD2 = 271.2 ± 42.9%, $P = 004$, $n = 8$; KD3 = 233.7 ± 40.3%, $P = 0.009$, $n = 8$, C = 100%). We confirmed that this increase is mainly due to an increase in SERCA2 expression. Figure 5D shows increased levels of isoform SERCA2 (KD1 = 189.8 ±

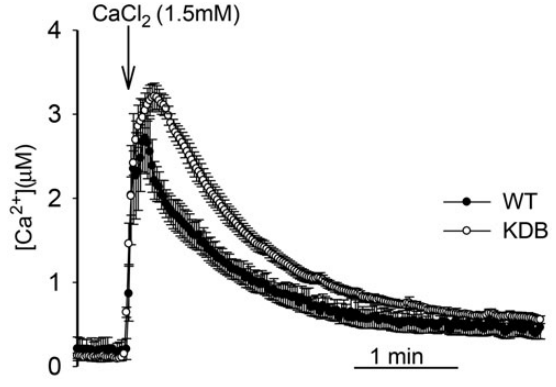

Figure 3. Changes in cytosolic free calcium concentration in wild-type MIN6 and Wolframin-depleted KDB cells. Cells were infected with adenovirus expressing untargeted (cytosolic) aequorin. Forty-eight hours later, cells were depleted of calcium (see 'Materials and Methods'), then perifused in nominally Ca^{2+}-free buffer, followed by buffer with 1.5 mmol/l $CaCl_2$ as indicated. The figure shows the results obtained over 2 days of experimentation (n, wt = 8, n, KDB = 9 runs).

Table 1. Total ATP content (relative luciferase units) of wild-type MIN6 and WFS1-depleted MIN6 cells

Cell line	RLU/104 cells ± SE	% (total ATP of wt)
pSuper (WT)	378 691.2 ± 9283	100
KDA	297 797.4 ± 10 111	78.6
KDB	198 801.5 ± 12 976	52.5

Total ATP content was assayed using CellTiter-Glo Luminescent Cell Viability Assay (Promega) as described under 'Material and Methods'. The results are presented as relative luciferase units (RLU) per 10^4 cells and as a per cent of ATP content in wild-type. The results come from three independent experiments with n wt = 72, n KDB = 66, n KDA = 72 (t-test: wt versus KDB, $P = 4.8 \times 10^{-21}$; wt versus KDA, $P = 1.0 \times 10^{-8}$).

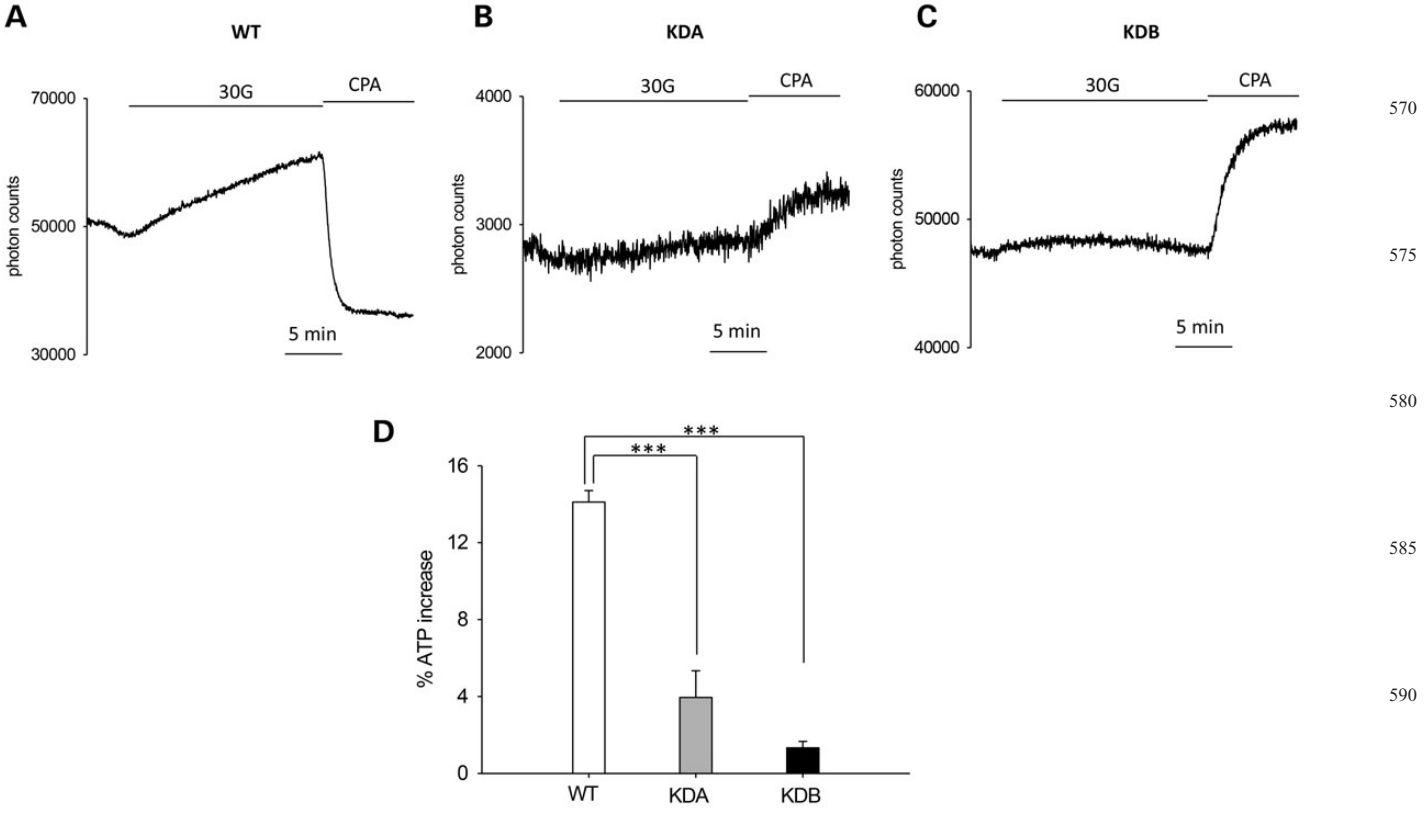

Figure 4. Glucose-induced cytosolic-free ATP changes in wild-type MIN6 and Wolframin-depleted cells. Cells were infected with adenovirus expressing cytosolic luciferase and, 48 h later, perifused in the presence of 5 μmol/l luciferin in a photon-counting device as described under 'Materials and Methods'. Representative traces for (**A**) wild-type MIN6 cells, (**B**) KDA and (**C**) KDB. The y axes represent photon counts, proportional to cytosolic ATP concentration ($[ATP]_{CYT}$) (23,24). Note the reduced ATP rise in response to 30 mmol/l glucose in WFS1-depleted cells. (**D**) Quantitative analysis of the glucose-induced rise in cytosolic ATP in wild-type MIN6 and WFS1-depleted cells. The percentage increase in apparent free cytosolic ATP concentration in response to elevated glucose was about 3-fold lower in KDA than in wild-type MIN6 (***wild-type versus KDA: $P = 7.43 \times 10^{-5}$) and about 10-fold lower in KDB than in wild-type MIN6 (***wild-type versus KDB: $P = 1.8 \times 10^{-13}$); n, wild-type = 12; n, KDA = 6 and n, KDB = 12 runs).

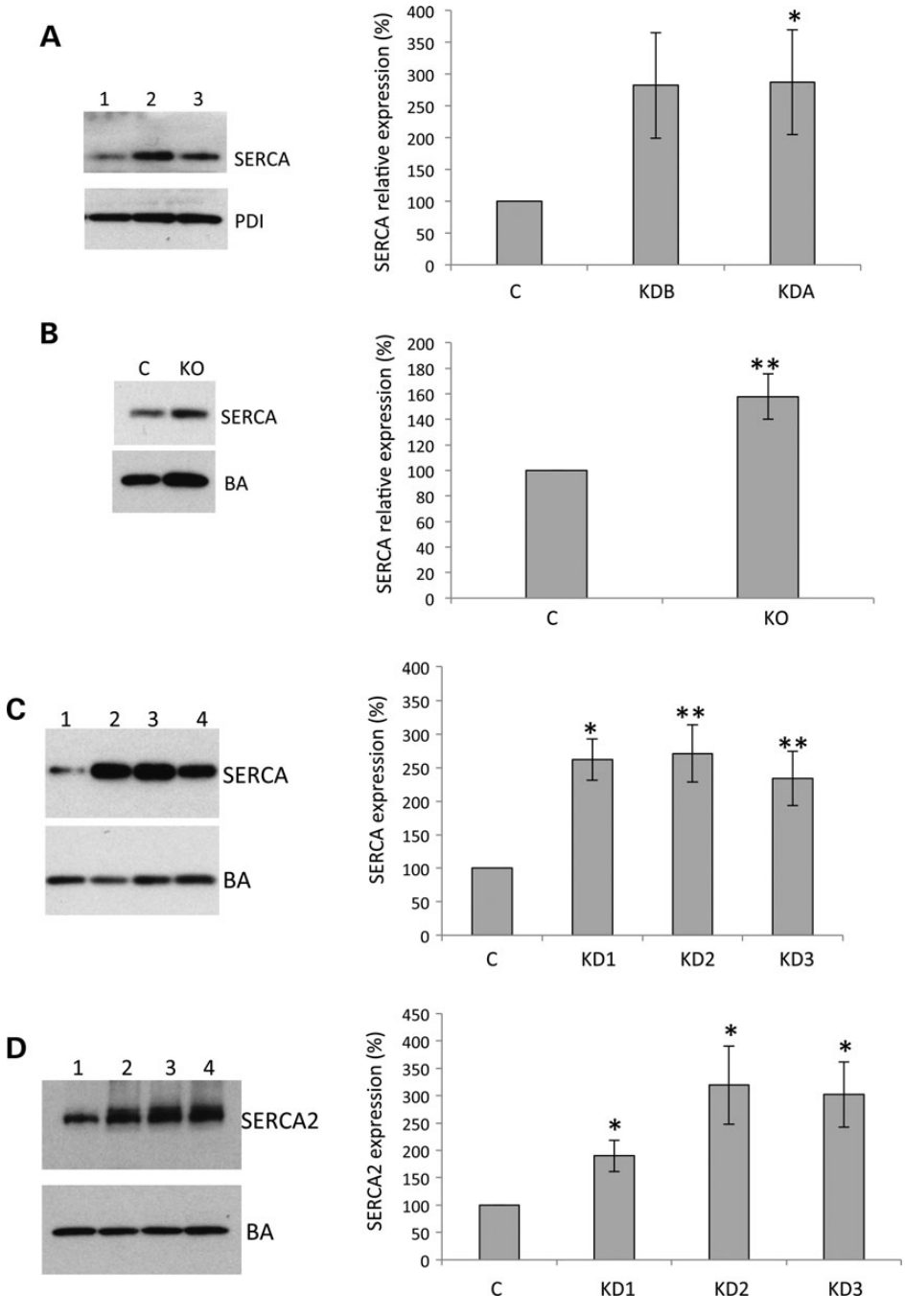

Figure 5. SERCA expression in WFS1-depleted cell models. Representative immunoblots and bar charts showing quantitative analysis. (**A**) SERCA expression in *WFS1*-depleted MIN6 cells—microsomal fractions. Immunoblot: lane 1control (C), lane 2 KDB, 3 KDA. Top panel: PanSERCA antibody Y1F4 (31) used for detection, bottom panel: PDI antibody used for normalization. Twenty-two micrograms of microsomal fraction extract was loaded per lane (*C versus KDA, $P = 0.045$, C versus KDB, $P = 0.052$, $n = 6$ runs with two independently prepared microsomal fraction extracts). (**B**) SERCA expression in primary islets isolated from *Wfs1* conditional KO mice-whole protein extracts. (**C versus KO, $P = 0.005$, $n = 4$, using two independently prepared extracts). Top panel: PanSERCA antibody Y1F4 (31), bottom panel: BA. Ten micrograms of protein extract were loaded per lane. (**C**) SERCA expression in *WFS1*-depleted neuroblastoma SK-N-AS cells, total protein extracts. Top panel: PanSERCA antibody Y1F4 (31), bottom panel: BA. (*C versus KD1: $P = 0.02$, $n = 3$; **C versus KD2: $P = 0.004$, $n = 8$; **C versus KD3: $P = 0.009$, $n = 8$). Two independently prepared KD1 extracts and, five independently prepared KD2 and KD3 extracts were run. Seventeen micrograms of protein extract was loaded per lane. Lanes: 1, control; 2, KD1; 3, KD2; 4, KD3. (**D**) Expression of SERCA2 isoform in *WFS1*-depleted neuroblastoma SK-N-AS cells—total protein extracts. Top panel: isoform SERCA2-specific antibody (Santa Cruz), bottom panel: BA. (*C versus KD1: $P = 0.04$, $n = 4$; C versus KD2: $P = 0.02$, $n = 6$; C versus KD3: $P = 0.02$, $n = 6$). Two independently prepared KD1 extracts and three independently prepared KD2 and KD3 extracts were run. Seventeen micrograms of protein extract were loaded per lane. Lanes: 1, control; 2, KD1; 3, KD2; 4, KD3.

28.6%, $P = 0.04$, $n = 4$; KD2 = 318.9 $\pm$ 71.2%, $P = 0.02$, $n = 6$; KD3 = 301.7 $\pm$ 59.3%, $P = 0.02$, $n = 6$, C = 100%).

In summary, all WFS-depleted models showed increased levels of SERCA expression (the main contributor being isoform SERCA2). This is consistent with our hypothesis that in WFS1-depleted cells SERCA may be overactive.

WFS1 interacts with SERCA2

To explain how the absence of WFS1 protein may affect the levels of SERCA expression, we hypothesized that the two proteins may be molecular partners. We first examined the potential WFS1–SERCA2 interaction in an over-expression system. We co-transfected FLAG-SERCA2 plasmid (constructed as described in 'Materials and Methods') together with Myc-WFS1 (20) or with the empty vectors to Cos7 cells. The following protein extracts were used: Myc-WFS1/FLAG-SERCA2, Myc-WFS1/empty FLAG, empty Myc/FLAG-SERCA2 and empty Myc/empty FLAG for immunoprecipitation with anti-FLAG antibody (Fig. 6A). Input panels at the left-hand side show the expression of relevant proteins in extracts before co-immunoprecipitation. Immunoprecipitation panels at the right-hand side show co-immunoprecipitation with mouse monoclonal anti-FLAG antibody probed with either anti c-myc (top panel) or anti-WFS1 antibody (middle panel). The results on Figure 6A show that with anti-FLAG antibody we were able to precipitate Myc-WFS1 (lane 1). No WFS1 was detected in lanes 2–4, where either Myc-WFS1/empty FLAG (lane 2), empty Myc /FLAG-SERCA2 (lane 3) or empty Myc/empty FLAG (lane 4) plasmids were present. We probed the membrane with polyclonal rabbit anti-FLAG antibody (bottom panel) to show the input.

In a reciprocal experiment (Fig. 6B, right-hand side panel), polyclonal rabbit anti c-myc antibody was used for co-immunoprecipitation and monoclonal mouse anti-FLAG antibody for detection (top panel). Only in lane 1, where both Myc-WFS1 and FLAG-SERCA2 proteins were expressed, we observed co-immunoprecipitation of FLAG-SERCA2. There

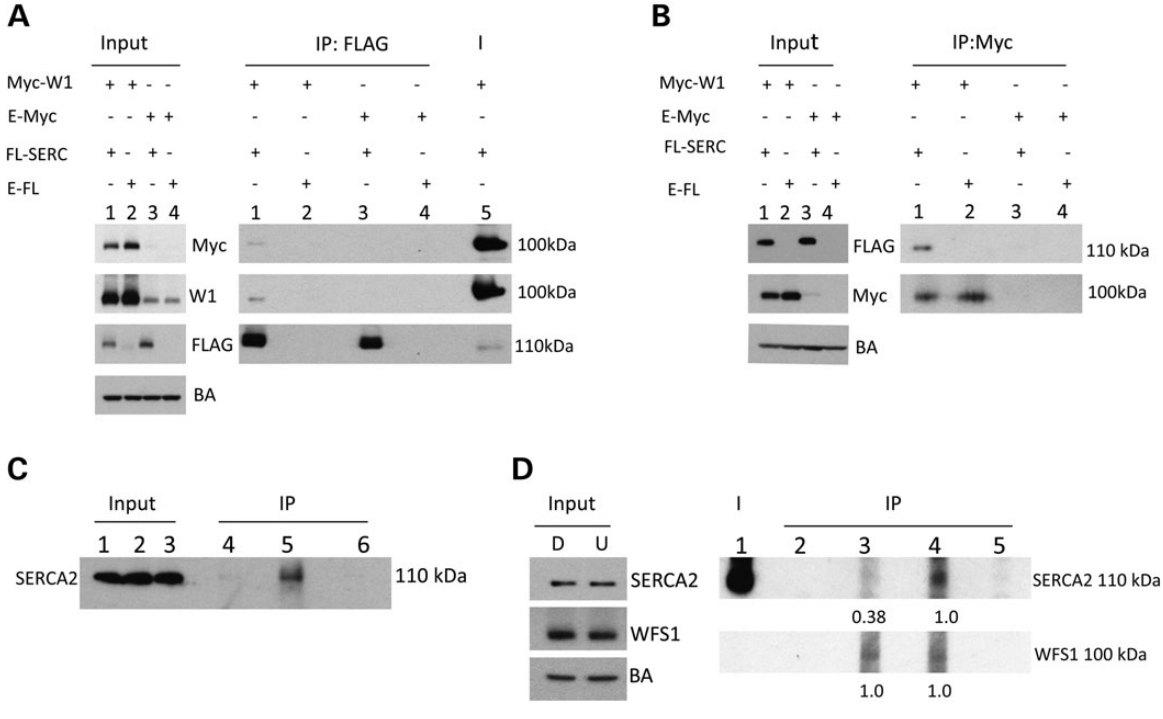

Figure 6. Co-immunoprecipitation of WFS1 and SERCA2. (**A** and **B**) Co-immunoprecipitation of WFS1 and SERCA2 in overexpressed system in Cos7 cells co-transfected with plasmids Myc-WFS1 and FLAG-SERCA2 or the relevant empty vectors as controls. (A) Right-hand side panels—IP: FLAG (immunoprecipitation with mouse monoclonal anti-FLAG antibody, immunoblotting with either c-myc antibody (rabbit polyclonal, Sigma, top panel), WFS1 antibody (rabbit polyclonal, middle panel) or FLAG (rabbit polyclonal, bottom panel). Panels at the left-hand side show the input: the expression of indicated proteins in extracts before co-immunoprecipitation (1% of extracts used in CO-IP). Lanes (on both: IP and input): 1, Myc-WFS1/FLAG-SERCA2; 2, Myc-WFS1/empty FLAG; 3, empty Myc/FLAG-SERCA2; 4, empty Myc/empty FLAG. Lane 5 (on Co-IP gel): input—extract expressing myc-WFS1 and FLAG-SERCA2. Myc-W1 = Myc-WFS1, FL-SERC = FLAG-SERCA2, E-Myc = empty vector Myc, E-FL = empty vector FLAG. (B) Right-hand side panels: IP: Myc—immunoprecipitation with c-myc antibody (rabbit polyclonal). Top panel: immunoblot with FLAG antibody (mouse monoclonal), bottom panel immunoblot with c-myc (mouse monoclonal). Panels at the left-hand side show the input: the expression of indicated proteins in extracts before co-immunoprecipitation (1% of extracts used in Co-IP). Lanes (on both: IP gel and input): 1, Myc-WFS1/FLAG-SERCA2; 2, Myc-WFS1/empty-FLAG; 3, empty Myc/FLAG-SERCA2 and 4, empty MYC/empty- FLAG. (**C**) Co-IP of endogenous WFS1 and SERCA2 from SK-N-AS cells with anti-WFS1 antibodies (rabbit polyclonal). Immunoblot: SERCA2 (goat polyclonal). Lanes 1–3: input (1% of extracts used for Co-IPs in lanes 4–6); lane 4: negative control: IP with anti-FLAG antibody (rabbit polyclonal); lane 5: IP with WFS1 antibody (rabbit polyclonal); lane 6: negative control: IP with FLAG antibody (mouse monoclonal), $n = 4$. (**D**) Co-IP of endogenous WFS1 and SERCA2 from SK-N-AS cells after DTT treatment ($n = 3$). Left panel: input-expression of SERCA2 and WFS1 in DTT treated (D) and untreated (U) extracts before immunoprecipitation; note that there is no decrease in expression levels for neither of the proteins. Right panel: IP. Lanes: 1, input (2.5% of extract used for IP); lanes 2 and 5, negative controls (IPs with FLAG antibody with untreated and treated extracts, respectively); lane 3: IP with WFS1 antibody from DTT-treated sample and lane 4, IP with WFS1 antibody from untreated sample. Top panel: immunoblotting with SERCA2 antibody, bottom panel: the same membrane probed with WFS1 antibody. Numbers below the gel panels show relative quantification of SERCA2 bands intensity normalized with WFS1.

was no SERCA2 detected in lanes 2–4, where either Myc-WFS1/empty FLAG (lane 2), empty Myc/FLAG-SERCA2 (lane 3) or empty Myc/empty FLAG (lane 4) were present. The bottom panel probed with monoclonal mouse c-myc antibody shows the input. These results indicate that WFS1 and SERCA2 can interact in an over-expression system.

Next we examined if endogenous WFS1 and SERCA2 can be co-immunoprecipitated from SK-N-AS neuroblastoma cells (Fig. 6C). WFS1 antibody (rabbit polyclonal) was used for precipitation (lane 5) and a ~110 kDa band was detected with SERCA2 antibody. No SERCA2 was detected in either lane 4 or 6 where negative controls, either FLAG- rabbit polyclonal or FLAG-mouse monoclonal antibody, were used for co-immunoprecipitation. Our results indicate that the two proteins WFS1 and SERCA2 may interact with each other in SK-N-AS neuroblastoma cells.

To understand the role of this interaction, we examined if WFS1 and SERCA2 can interact with each other under conditions of ER stress. We prepared protein extracts from neuroblastoma SK-N-AS cells either untreated or treated with ER stress inducer: 1 mmol/l dithiothreitol (DTT) for 3 h. First, we examined the expression of both proteins in these extracts (Fig. 6D, left panel): the expression levels of SERCA2 were slightly elevated in DTT treated extract (D) in comparison to untreated (U) (D: 134.8 ± 8.1%, U: 100%, $P = 0.02$, $n = 4$), WFS1 levels were unchanged by the treatment: (D: 97.8 ± 6.3%, U = 100%, $P = 0.75$, $n = 4$). In summary, there was no decrease in the expression of either of these two proteins upon DTT treatment (Fig. 6D, left panel). Then, we performed co-immunoprecipitation of SERCA2 with rabbit WFS1 antibody (Fig. 6D, right panel, $n = 3$) using either DTT treated extract (lane 3), or untreated extract (lane 4). We detected the presence of SERCA2 band in lane 4 (top panel), where untreated extract was used. Interestingly, the SERCA2 band in the DTT-treated sample was much reduced (Fig. 6D, lane 3, top panel). The membrane was re-probed with sheep WFS1 antibody and the amount of precipitated WFS1 quantified showing equal amounts in both DTT treated and untreated samples (DTT: 1.0, untreated: 1.0, Fig. 6D, lower panel). Next, the amount of precipitated SERCA2 was quantified and normalized for the WFS1 levels: (untreated sample: SERCA2 = 1.0; DTT treated sample: SERCA = 0.38). In summary, DTT treatment did not affect either the protein expression or the amounts of precipitated WFS1 (Fig. 6D). This suggests that the 62% reduced levels of the amount of precipitated SERCA2 in DTT-treated sample do not result from reduced levels of precipitated WFS1 under these conditions. Our results thus suggest that WFS1–SERCA2 interaction may be impaired under ER stress conditions.

Proteasome inhibition results in an increase of SERCA2 levels in a WFS1-dependent manner

We demonstrated above that WFS1 interacts with SERCA and SERCA expression is increased in WFS1-depleted cells. We hypothesized that WFS1 may be a negative regulator of SERCA and targets SERCA to proteasome-mediated degradation. To test our hypothesis, we compared SERCA levels in control and the WFS1-depleted cell line KD2 after treatment with the proteasome inhibitor MG132. Control and WFS1-depleted KD2 cells were treated with either 5 or 10 μmol/l MG132 proteasome inhibitor as described by Gharanei *et al.* (21). Equal amounts of protein (11 μg) were loaded per lane and samples were resolved on sodium dodecyl sulphate polyacrylamide gel electrophoresis (SDS-PAGE) gels. SERCA expression in a DMSO-treated sample was assumed to be equal to 100%. Quantification revealed that while in control cells SERCA expression at 5 μmol/l increased to 226.9 ± 26.5% and at 10 μmol/l increase to 266.3 ± 51.9% (2.2- and 2.6-fold, respectively, $n = 6$) the increase of SERCA expression was much reduced in KD2 cells to 125.0 ± 8.9% at 5 μmol/l and 106.7 ± 24.3% at 10 μmol/l (1.2- and 1.1-fold, respectively, $n = 4$). The difference in accumulation of SERCA between control and KD2 cells was statistically significant: C versus KD2 at 5 μmol/l: $P = 0.01$; C versus KD2 at 10 μmol/l: $P = 0.03$, $n = 6$ (Fig. 7). This result together with the previously demonstrated interaction between the two proteins and significantly

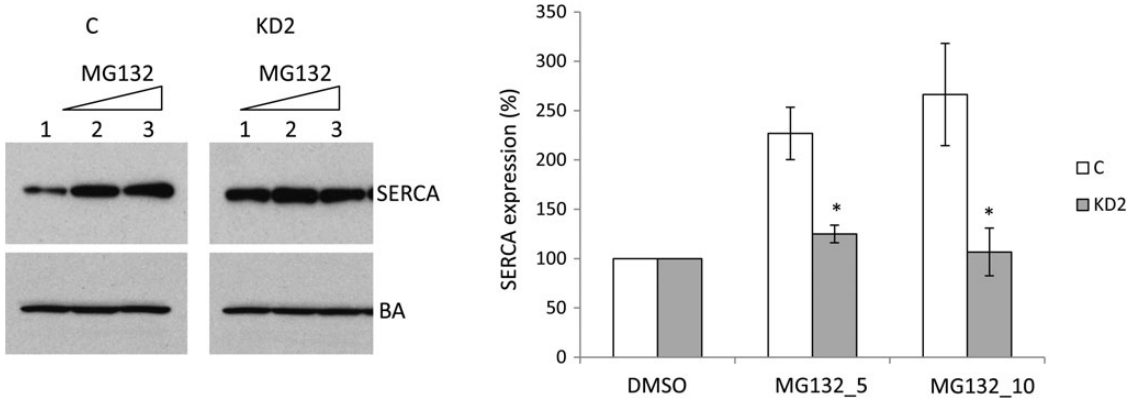

Figure 7. Proteasome inhibition results in an increase of SERCA levels in WFS1-dependent manner. Control (C) and WFS1-depleted (KD2) neuroblastoma (SK-N-AS) cells were grown for 24 h in six-well plates and then treated with MG132 proteasome inhibitor (5 or 10 μmol/l) for 4 h before being harvested for protein analysis. The control samples were treated with equal volume of DMSO. The expression of SERCA was measured by western blotting using PanSERCA antibody Y1F4 (31) and normalized to BA. Eleven grams of protein extract was loaded per lane. Lanes (both panels): 1, DMSO: treatment; 2, MG132 at 5 μmol/l and 3, MG132 at 10 μmol/l. Bar chart—quantification of SERCA expression: (*C versus KD2 at 5 μmol/l MG132: $P = 0.01$; C versus KD2 at 10 μm/l MG132: $P = 0.03$; control $n = 6$ runs, KD2, $n = 4$ runs using two independently treated extracts). MG132_5: treatment with 5 μmol/l MG132; MG132_10: MG132 at 10 μmol/l.

increased SERCA levels in WFS1-depleted cell model is consistent with the possibility that WFS1 targets SERCA to the proteasome for degradation. However, the ubiquitination assay, in which we compared SERCA ubiquitination levels between KD2 and control cells did not show impaired SERCA ubiquitination in KD2.

DISCUSSION

In Wolfram syndrome, diabetes mellitus results from multiple defects in the glucose signalling pathway; and both the diabetes mellitus and neurodegeneration are thought to be associated with ER calcium depletion. This study provides additional insights into its role in both mouse pancreatic beta-cell and human neuroblastoma cell models of the disease. We observed the following: (1) our models confirmed that WFS1 protein depletion in MIN6 beta-cells and primary islets resulted in reduced glucose-stimulated insulin secretion, and reduced and delayed cytosolic Ca^{2+} rise to glucose; (2) we observed a reduced cytosolic ATP rise in response to high glucose, and reduced total cellular ATP content; (3) SERCA expression levels were increased in WFS1 protein-depleted MIN6 cells, WFS1 KO primary islets, and WFS1 protein-depleted human neuroblastoma cells; (4) WFS1 protein interacted with SERCA in both overexpressed and endogenous models; (5) proteasomal inhibition studies suggested a role for WFS1 in SERCA protein turnover and (6) when ER stress was induced with DTT, there was a reduced WFS1/SERCA complex formation or partial dissociation, allowing SERCA expression to increase. These results are consistent with a model in which WFS1 protein negatively regulates the ER stress response and modulates ER calcium filling by regulating SERCA expression to partially compensate for ER calcium depletion in conditions of ER stress.

We showed that in two MIN6 beta-cell models of Wolframin depletion, there was reduced glucose-stimulated insulin secretion (Fig. 1A). We also demonstrated the defect in glucose-stimulated insulin secretion in primary islets isolated from conditional beta-cell-specific KO mice (Fig. 1B). In our MIN6 model of Wolframin depletion, this was associated with a delayed and reduced amplitude of the $[Ca^{2+}]_i$ rise (Fig. 2), and reduced $[ATP]_{CYT}$ rise in response to elevated glucose (Fig. 4). These findings thus confirm and extend previous observations of multiple defects in the control of glucose signalling and insulin secretion in Wolframin-depleted beta-cells (16,17,22).

Our findings of reduced $[ATP]_{CYT}$ rise in response to elevated glucose, and reduced total cellular ATP, suggest reduced ATP synthesis or increased ATP consumption after WFS1 silencing (23,28). This reduced $[ATP]_{CYT}$ rise may explain the observed reduced and delayed glucose-induced $[Ca^{2+}]_i$ rise in these mutants (due to failed closure of ATP-sensitive K^+ channels). ATP generation defects have not been previously reported in Wolfram syndrome; our own previous work demonstrated normal oxidative phosphorylation in muscle biopsies from Wolfram patients (30). Increased ATP consumption could arise from cellular efforts to restore ER homeostasis. SERCA pump activity has been shown to be a major ATP-consuming process in MIN6 cells (28) and has also been proposed as a negative regulator of $[ATP]_{CYT}$, contributing to the Ca^{2+}-dependent oscillations in $[ATP]_{CYT}$ observed in beta-cells (33,34).

These observations led us to hypothesize that ATP utilization by SERCA may increase in the absence of WFS1 protein; and further, that increased activity/expression of SERCA would be observed in WFS1 protein depletion. To test our hypothesis, we studied the levels of SERCA expression in several models of WFS1-depleted cells: pancreatic MIN6, SK-N-AS neuroblastoma and in primary islets isolated from *WFS1* conditional KO mice. All our models showed elevated ER stress markers (16,21). We found that SERCA levels were significantly elevated in all our models and that it was mainly due to increased levels of isoform SERCA2 (Fig. 5). This is a novel finding and to the best of our knowledge, there are no published reports of SERCA expression in WFS1 protein-depleted cell models.

We demonstrated that WFS1 and SERCA interact in both an over-expression system (Fig. 6A and B) and endogenously (Fig. 6C); and that this interaction is reduced in the presence of DTT-induced ER stress (Fig. 6D). Inhibition of the proteasome with MG132 resulted in accumulation of SERCA in a WFS1-dependent manner: the accumulation of SERCA expression was reduced in WFS1-depleted neuroblastoma cell line KD2 in comparison to WFS1 positive control (Fig. 7). These results suggested that WFS1 may be a negative regulator of SERCA and were consistent with the possibility that the WFS1–SERCA interaction regulates SERCA levels by targeting SERCA to degradation by the proteasome. Our ubiquitination study did not confirm impaired SERCA ubiquitination in WFS1-depleted cells (data not shown). We tested for 'canonical' signals for proteasomal recognition with antibody against ubiquitin lysine-48 based chains. However, several 'non-canonical' ubiquitin-based signals for proteasomal targeting have also been described (e.g. polyubiquitin chains assembled through residues other than lysine 48), tagging substrates with 'ubiquitin-like' proteins or proteasomal degradation without prior ubiquitination (35). Therefore, the mechanism of WFS1 regulation of SERCA requires further confirmation.

It seems that the regulation of SERCA protein levels by WFS1 may be ER stress dependent: under conditions of ER stress SERCA is released from the interaction with WFS1 (or alternatively SERCA–WFS1 complexes are formed at a lower rate), it may be degraded by the proteasome to a lesser extent, and SERCA expression increases. Under normal conditions of ER homeostasis, the physiological levels of SERCA may be maintained in homeostasis by interaction with WFS1. A similar function for WFS1 was described by Fonseca *et al*. (15) who demonstrated that WFS1 negatively regulates a key transcription factor involved in ER stress signalling activating transcription factor 6α (ATF6α) through the ubiquitin-proteasome pathway.

Some forms of ER stress result in ER calcium depletion, disturbed ER functions and increase in cytosolic calcium levels, which may trigger cell death via activation of the calpain-2 apoptotic pathway (7). We provide evidence that under conditions of WFS1 protein depletion, there may be a secondary increase in SERCA expression to pump calcium ions back into the ER calcium store to try to restore ER homeostasis. Several reports show that induction of ER stress may lead to increased SERCA expression on both mRNA and protein levels (11,36–39). In addition, Wu *et al*. (40) reported that cytosolic calcium elevation itself increased SERCA2 expression by a mechanism distinct from ER stress. The authors speculated that enhanced calcium uptake into the ER might shorten the

period of a relative ER calcium depletion subsequent to a stimulus-induced ER calcium release, in this way responding to an increased demand for calcium by ER chaperones system under the conditions where unfolded proteins can be accumulated. In contrast, other authors have reported that under pathological conditions associated with cell death, including ER stress, SERCA expression is decreased (7,41,42). The discrepancy may relate to the degree of ER stress: in resolvable ER stress, SERCA expression and function may increase to restore ER calcium levels; in irresolvable ER stress, ER calcium levels cannot be restored SERCA expression falls and apoptosis ensues.

The absence of WFS1 is associated with ER stress (14–17), calcium leak from the ER and an elevation of cytosolic calcium levels (7). ER stress, ER calcium leak and elevations of cytosolic calcium have all been associated with increases in SERCA expression (11,36–38,40). ATF6 is also negatively regulated by WFS1, and a downstream effect of increased ATF6 activity is elevation of SERCA expression (11). It may be that under these conditions for the cells to survive SERCA expression must be increased to counteract the ER calcium leak to restore ER calcium homeostasis and to prevent activation of cell death pathway induced by elevated cytosolic calcium levels. The decrease of SERCA levels under ER stress and under some pathological conditions observed by Hara *et al*. (7) was in the presence of WFS1, where induction of this compensatory mechanism was not necessary; WFS1 exerted its pro-survival function and prevented cell death. Our results, summarized on Figure 8, are consistent with the possibility that WFS1 negatively regulates SERCA turnover, possibly via proteasome-mediated degradation and this process is dependent on the ER stress. Release of SERCA from interaction with WFS1 in WFS1-depleted cells or under ER stress may result in increased SERCA levels and activity and may allow compensatory pumping of calcium ions from cytosol to ER lumen to restore ER calcium homeostasis and prevent cell death.

To further understand WFS1 role in calcium homeostasis, it will be interesting to examine if/how WFS1 depletion affects the expression of IP3R and RYR, the calcium channels that release calcium from the ER and how WFS1 depletion affects other intracellular Ca^{2+} stores.

In summary, our results support previously reported WFS1 involvement in regulation of glucose sensing and insulin secretion in pancreatic cells and demonstrate for the first time a defective ATP response to glucose and ATP depletion in the absence of WFS1. We also demonstrate that WFS1 is an interactive partner and a negative regulator of SERCA.

MATERIALS AND METHODS

Cell culture and adenoviral infection

Mouse beta-cell-derived MIN6 cells expressing interfering RNAs to provide reduction in *WFS1* expression (16) were

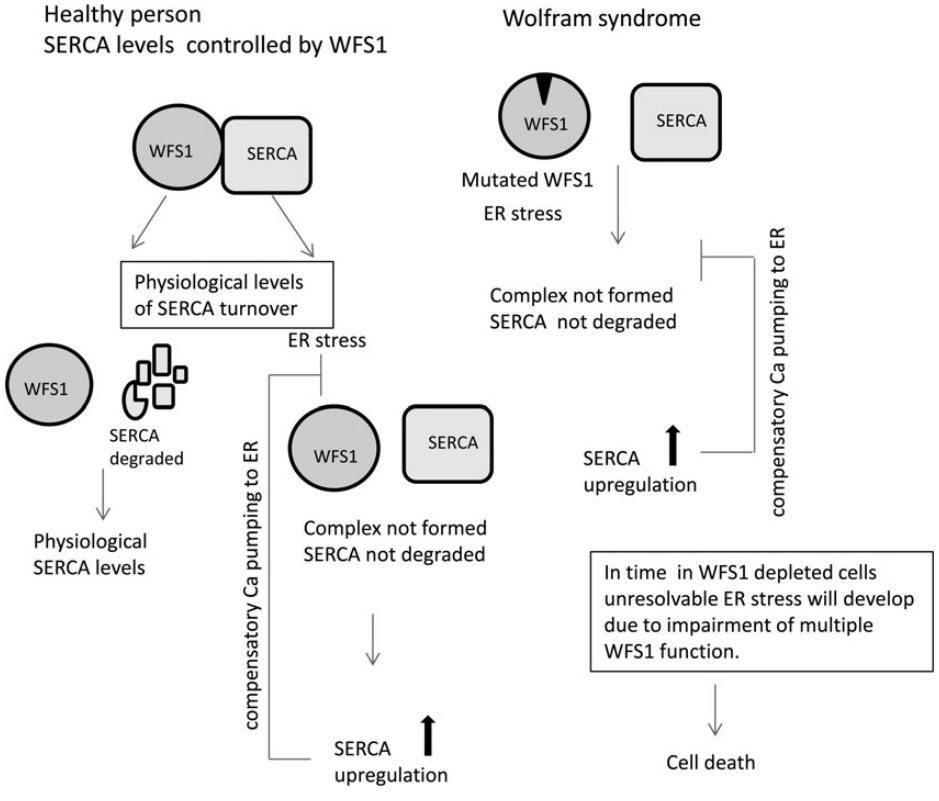

Figure 8. Regulation of ER calcium homeostasis by WFS1 via regulation of SERCA2 levels: under conditions of calcium homeostasis (normal conditions) WFS1 interacts with SERCA and negatively regulates SERCA turnover to maintain physiological SERCA2 levels. Under conditions of ER stress or in WFS1-depleted cells, WFS1–SERCA2 interaction is limited: the complex is either not formed or formed at a reduced level. This results in SERCA2 upregulation. SERCA2 upregulation provides a compensatory mechanism, which allows for increased Ca^{2+} pumping to the ER in response to Ca^{2+} leak from the ER caused by either ER stress or WFS1 depletion. This compensatory mechanism allows restoration of calcium homeostasis and prevention of cell death.

cultured in Dulbecco's modified Eagle's medium (Sigma) containing 25 mmol/l glucose, 2 mmol/l pyruvate, supplemented with 15% (vol/vol) foetal bovine serum, 4 mmol/l glutamine, 100 units/ml penicillin, 100 μg/ml streptomycin, 143 μmol/l β-mecaptoethanol and 0.2 mg/ml geneticin. Luciferase expression was achieved by infection of cells with adenoviral vector encoding cytoplasmic-targeted luciferase (AdCMVcLuc) (23), aequorin expression by using untargeted cytosolic aequorin (Cyt.Aq) (43). Human neuroblastoma SK-N-AS cells with stable WFS1 depletion were grown as described by Gharanei *et al*. (21).

Insulin secretion from MIN6 cells

Cells were seeded in six-well plates and grown in full growth medium for at least 16 h, before they were maintained overnight in medium with 3 mmol/l glucose. Insulin secretion was performed as previously described (http://www.jbc.org/content/280/27/25565.long) and insulin content measured by radioimmunoassay (Millipore).

Isolation of pancreatic islets, insulin secretion assay and preparation of protein extracts

The mice used in this experiment were beta-cells selective conditional *Wfs1* KO mice (16), obtained by collaboration from Professor A. Permutt. They were additionally back crossed with C57 wild-type females for two generations and the heterozygotes were used as parents in matings to obtain experimental and control littermates. Islets were isolated by collagenase digestion from pancreata of 10–13 weeks old male mice: either *Wfs1* conditional KO mice ($Wfs1^{fl/fl}$ $Cre^{cre/+}$) or *Wfs1* positive 'floxed' littermates ($Wfs1^{fl/fl}$). Islets of Langerhans were isolated, cultured and insulin secretion assay performed as previously described (27,44).

For preparation of protein lysates for immunoblotting the islet was incubated in RPMI medium for 10–12 days, handpicked every other day and lysed in RIPA buffer (400–500 islets were lysed in 60–70 μl of buffer). For homogenization, the lysate was multiple times frozen (at −80C) and defrosted at RT, each time being passed several times through a pipette tip followed by passing through a 21.5G size needle (27,44).

Cytosolic free Ca^{2+} concentration measurements with fura-2

Cells were seeded on 24 mm diameter coverslips and starved in medium containing 3 mmol/l glucose overnight. The next day, cells were loaded with the fluorescent dye fura-2 (5 μmol/l) and incubated in Krebs buffer (see above) with 3 mmol/l glucose. Next, the cells were perifused with buffer containing 3 mM glucose followed by 30 mmol/l glucose, then 50 mmol/l KCl as a control. Changes in ($[Ca^{2+}]_i$) in single cells were measured as the changes in fluorescence intensity of fura-2 using an Olympus IX-80 inverted optics epifluorescence microscope (×40 oil immersion objective). Single cell $[Ca^{2+}]_i$ measurements were performed exciting the dye at 340 and 380 nm, and emission was recorded at 510 nm. Images were recorded with an IMAGO charge-coupled device camera (Till Photonics GmbH, Grafelfing, Germany) controlled by Tillvision software (Till Photonics).

Measurements of cytosolic free Ca^{2+} with recombinant targeted aequorin

Cells were seeded onto 13 mm diameter coverslips and 24 h later, at 70–80% confluency, transfected with adenoviruses expressing the untargeted (cytosolic) bioluminescent protein aequorin (45,46). Forty eight hours later, cells were depleted of Ca^{2+} by incubation with 10 μmol/l ionomycin, 10 μmol/l CPA and 10 μmol/l monensin in modified Krebs-Ringer bicarbonate buffer containing glucose 3 mmol/l, Hepes 10 mmol/l, KCl 3.5 mmol/l, $MgSO_4$ 0.5 mmol/l, NaCl 140 mmol/l, $NaHCO_3$ 2 mmol/l and NaH_2PO_4 0.5 mmol/l (to achieve pH 7.4) and supplemented with EGTA 1 mmol/l for 5 min at 4C (46). Cytosolic free calcium levels were measured using a cytoplasmic (non-targeted) aequorin construct and native coelenterazine (47). Aequorin was reconstituted with 5 μmol/l coelenterazine in Krebs buffer with 0.1 mmol/l EGTA for 2 h at 4°C (48). The cells were perifused with Ca^{2+}-free buffer, followed by addition of buffer containing 1.5 mmol/l $CaCl_2$ at 120 s to permit Ca^{2+} entry. The photon counts were detected with a photomultiplier device (Thorn EMI) (49) adjacent to the perifusion chamber and converted to Ca^{2+} concentration (μmol/l) using algorithms described previously (50,51).

Cytosol free ATP concentration measurements

Cells were seeded onto 13 mm diameter coverslips and 24 h later, at 70–80% confluency infected with adenovirus expressing untargeted (cytosolic) firefly luciferase (23,24). After 48 h culture, the cells were 'starved' overnight in medium containing 3 mmol/l glucose. The following day, the cells were incubated for a further 15 min in modified Krebs buffer containing 3 mmol/l glucose, then perifused in the same buffer containing 3 mmol/l glucose, followed by buffer with 30 mmol/l glucose and then followed by addition of CPA (10 μmol/l), an inhibitor of SERCA. The cytosolic free ATP concentration ($[ATP]_{CYT}$) was estimated by counting the emitted photons with a photomultiplier as described above.

Measurements of ATP:ADP ratio in response to rise in glucose concentration

Cells were seeded in six-well plates in standard media. The next day the cells were starved overnight in the medium with 3 mmol/l glucose. On the day of experiment, the cells were incubated for 15 min in Krebs buffer with 3 mmol/l glucose; and after that they were incubated for 15 min in Krebs buffer with either 3 mmol/l glucose (plate 1), 30 mmol/l glucose (plate 2) or 30 mmol/l glucose and CPA (plate 3). The plates 1 and 2 were harvested after 15 min in 200 μl per well of 20% (v/v) ice-cold PCA and rapidly frozen in −80°C. 10 μmol/l CPA was added to plate 3 and incubated additional 5 min before being harvested in PCA as above. In parallel, another plate was seeded in an identical way for measurements of protein concentration to normalize the results and harvested in protein lysis buffer (RIPA). A standard curve for ATP and ADP (a negative control) was prepared (gradient of concentrations versus luminescence). The samples

(harvested in PCA) were neutralized to pH 7.4 with a known volume of neutralization mixture (0.5 mol/l triethanolamine, 2 mol/l KOH and 100 mmol/l EDTA). The samples were mixed with an aliquot of a reaction buffer containing sodium arsenate (65 mmol/l, pH7.4), $MgSO_4$ (20 mmol/l), KCl (5 mmol/l) and phosphoenolpyruvate (PEP). For each sample, two assays were performed: set 1 = ATP measurement with 'mock conversion' of ADP (in the reaction buffer as stated above, without pyruvate kinase) and set 2 = ATP + ADP measurement where ADP was converted to ATP by addition of pyruvate kinase. After 2 h incubation at RT, 10 μg of luciferase and 1 mmol/l luciferin were added to each sample and luminescence was measured on a luminometer for both: set 1 (ATP) and set 2 (ATP + ADP). The amount of ADP was calculated as a difference, ADP = (ATP + ADP) − ATP (29).

Total cellular ATP content

Cells were grown to 90% confluency in standard medium (see above) with 25 mmol/l glucose, harvested, diluted 10× in growing medium, counted and seeded in opaque-walled 96 wells plates (Appleton Woods). The following day total ATP assay was performed using the CellTiter-Glo Luminescent Cell Viability Assay (Promega). Briefly, the plates were equilibrated to room temperature for 30 min, and a volume of reconstituted CellTiter-Glo Reagent (100−100 μl of medium in each well) was added. The content was mixed for 2 min in an orbital shaker to induce lysis; after 10 min incubation in room temperature the luminescence was read on a multilabel counter Wallac 1420 Victor3 (Perkin Elmer).

Preparation of microsomal fractions

8 × T75 cm flasks of each wt, KDA and KDB MIN6 (80% confluent) were harvested by trypsinization, rinsed with phosphate buffered saline (PBS) and resuspended in 2 ml of PBS on ice. Cells were spun down at 2000 rpm, 5 min, 4°C and suspended in 10 ml of MEMBRANE buffer (5 mM HEPES, 0.32 M sucrose, pH 7.2 with protease inhibitors) before they were homogenized using electric homogenizer Polytron, ultra Turro T8 at 30 000 rpm for 10 s. Then, cells were transferred to a glass electric homogenizer and homogenized with 10 strokes. Cells were spun down at 10 000g, 10 min, 4°C to remove organelles (nuclei and mitochondria). Cloudy supernatant (15 ml) was harvested to a separate tube, divided between two ultracentrifuge tubes (3/4 full) and spun down at 100 000g for 1 h at 4°C.

Pellet (microsomes) was harvested by pouring off supernatant and resuspending in 500 μl each in MEMBR ANE buffer, no protease inhibitors cocktail. Aliquots of 100 μl were frozen in liquid nitrogen and transferred to a −70°C deep freezer immediately (32).

Proteasome inhibition assay

Cells were plated at 5×10^5 cells/well in a 6-well plate. After 24 h, cells were treated with either 5 or 10 μmol/l MG132 proteasome inhibitor for 4 h, harvested in RIPA buffer and prepared for western blotting as described by Gharanei *et al*. (21).

Immunoblotting

Antibody was diluted in 5% milk in PBS-Tween and used at the following concentrations: PanSERCA Y1F4 (mouse monoclonal (31)) 1:5000; SERCA2 (goat polyclonal Santa Cruz) 1:1000; BA (mouse monoclonal Sigma) 1:14 000 and PDI (mouse monoclonal Abcam) 1:5000. For protein detection in extracts from isolated islets the following concentrations of primary antibody were used: WFS1 (rabbit polyclonal, obtained by collaboration (20)) 1:500; PanSERCA Y1F4 1:500, BA 1:3500. Secondary antibody (anti-rabbit, goat and mouse, Dako) was used at 1:20 000.

Co-immunoprecipitation

Construction of FLAG-SERCA2 plasmid

Full length human SERCA2 (transcript variant b, GeneBank NM_170665.3) was amplified from a human cDNA library by polymerase chain reaction using primers 5′-CTTGCGGCCG CGATGGAGAACGCGCAC-3′ (forward) and 5′-GCATGGT ACCTCAAGACCAGAAGATATCG-3′ (reverse) and was cloned between the Not I and Kpn I site of pFLAG-CMV4 expression vector (Sigma). The sequence was confirmed by DNA sequencing. pCMV-Myc-WFS1 plasmid was described before (20).

Transfection

Cos7 cells were seeded at 2.0×10^6 in 10 cm plates and after 24 h co-transfected with the following combinations of plasmids (2 μg of each): pCMV-Myc-WFS1/FLAG-SERCA2, pCMV-Myc-WFS1/empty FLAG, empty Myc/FLAG-SERCA2 and empty Myc/empty FLAG using Turbofect transfection reagent (Thermo Scientific) according to manufacturer's instructions. After 48 h, the cells were harvested in 600 μl of RIPA buffer (20), sonicated 3 × 10 s and centrifuged at 23 000 g at 4°C.

Immunoprecipitation in over-expression system

A total of 750 μg of protein extract and either anti-FLAG mouse monoclonal antibody (Sigma) or anti c-myc rabbit, polyclonal antibody (Sigma), were used for co-immunoprecipitation in the over-expression system. The extracts were incubated with antibody overnight at 4°C with end-to-end rotation. Protein G Sepharose beads were added after overnight incubation for a further 4 h of end-to-end rotation at 4°C. Beads were separated from lysate using Spin-X columns (Costar) by centrifugation at 4000g for 15 min at 4°C and washed four times with RIPA buffer (for washes: 1, 2 and 4 RIPA buffer with 150 mmol/l NaCl was used, for wash 3 RIPA buffer with NaCl increased to 500 mmol/l was used). Each wash was performed by 15 min incubation at 4°C with end-to-end rotation, followed by spin at 4000g. Bound proteins were eluted in 50 μl sample buffer by heating to 70°C for 8 min followed by 3 min spin at a maximum speed in a microfuge and stored in −80°C. The following antibody was used for immunoblotting: c-myc (rabbit polyclonal, Sigma) 1:10 000; WFS1 (rabbit polyclonal, Proteintech) 1: 500; FLAG (rabbit polyclonal Sigma) 1:1000; FLAG (mouse monoclonal, Sigma) 1:1000 and c-myc (mouse monoclonal Sigma) 1:1000. Secondary anti-mouse and anti-rabbit antibody (Dako) were used 1:20 000.

DTT treatment

Eighty percentage confluent SK-N-AS cells growing in 10 cm dishes were treated with 1 mmol/l DTT (Sigma) for 3 h or remained untreated before being harvested in 600 μl Tris buffer (TBD, composition below). Equal amounts of untreated and DTT-treated protein lysates were used for co-immunoprecipitation as described below.

Immunoprecipitation of endogenous proteins

To detect endogenous interaction neuroblastoma SK-N-AS cells in 10 cm dishes were harvested in 600 μl TBD per dish [20 mmol/l Tris, pH 7.5, with 100 mmol/l NaCl, 1% TritonX-100, 1 mmol/l DTT, 1 mmol/l PMSF and protease inhibitors (Complete Mini, Roche)], scraped on ice, placed in eppendorfs and incubated at 4°C with end-to-end rotation for 1 h. The samples were sonicated 3 × 10 s on ice and the lysates cleared by centrifugation at 23 000 g at 4°C. 900 μg−1 mg of protein extract (400 μl) were used per reaction. WFS1 rabbit polyclonal antibody (Abcam) was used for co-immunoprecipitation and FLAG rabbit, polyclonal antibody (Proteintech) or FLAG mouse monoclonal antibody (Sigma) was used as negative control. After overnight incubation with the antibody, the lysates were transferred to Spin-X columns (Costar) with 20 μl of pre-cleared Protein G Sepharose beads, for 3 h incubation at 4°C with end-to-end rotation. The samples were centrifuged at 4000g at 4°C and the beads washed 2× in 400 μl of buffer TBD-150 (with 150 mmol/l NaCl), 1× in TBD-500 (with 500 mmol/l NaCl) and again 1× in TBD-150. Each time the beads were incubated 15–20 min at 4°C with end-to-end rotation. Finally, beads were separated from lysates by centrifugation at 4000 *g* and 50 μl of SDS loading buffer was added per sample. The proteins were released from beads by heating to 70°C for 8 min, spun down at 13 000 rpm in a microfuge for 3 min and supernatant harvested. The samples were run on SDS-PAGE gels, transferred to membranes at (90 V for 90 min) and boiled for 4 min in water before being blocked in 5% milk in PBS-Tween for 1 h. The membranes were incubated with SERCA2 goat polyclonal antibody (Santa Cruz) 1:1000 followed by anti-goat secondary antibody (Dako) 1:20 000, or WFS1 sheep polyclonal antibody (R&D systems) 1:10 000 followed by secondary anti-sheep (R&D systems) 1:30 000 overnight at 4°C with rotation.

Statistical analysis

Data are given as the means ± SE for the number of experiments given. Comparisons between means were performed using Student's *t*-test with Bonferroni correction for multiple testing, as appropriate.

ACKNOWLEDGEMENTS

The authors thank Dr Boris Kysela for kind advice on co-immunoprecipitation conditions.

Conflicts of Interest statement. The corresponding author confirms on behalf of all authors that there are no conflicts of interest to declare.

FUNDING

This was funded by grants to G.A.R. from the Wellcome Trust (Programmes 067081/Z/02/Z and 081958/Z/07/Z), Medical Research Council (90401641), European Union (FP6 'Save-beta') and an Imperial College Divisional Studentship to E.A.B. M.Z. is supported by The Birmingham Children's Hospital Research Foundation, Thames Honda and Wellchild. M.Z. is the recipient of a Wellcome Trust VIP award. Patient engagement was through the EURO-WABB project (www.euro-wabb.org) funded by The European Commission Health Programme Framework (2010 12 05), delivered through The NIHR Wellcome Clinical Research Facility, Birmingham.

REFERENCES

1. Ilieva, E., Ayala, V., Jové, M., Dalfó, E., Cacabelos, D., Povedano, M., Bellmunt, M., Ferrer, I., Pamplona, R. and Portero-Otín, M. (2007) Oxidative and endoplasmic reticulum stress interplay in sporadic amyotrophic lateral sclerosis. *Brain*, **130**, 3111–3123.
2. Hoozemans, J., van Haastert, E., Nijholt, D., Rozemuller, A. and Scheper, W. (2007) Activation of the unfolded protein response is an early event in Alzheimer's and Parkinson's disease. *Neurodegener. Dis.*, **10**, 212–215.
3. Cardozo, A., Ortis, F., Storling, J., Feng, Y., Rasschaert, J., Tonnesen, M., Van Eylen, F., Mandrup-Poulsen, T., Herchuelz, A. and Eizirik, D. (2005) Cytokines downregulate the sarcoendoplasmic reticulum pump Ca^{2+} ATPase 2b and deplete endoplasmic reticulum Ca^{2+}, leading to induction of endoplasmic reticulum stress in pancreatic beta-cells. *Diabetes*, **54**, 452–461.
4. Gwiazda, K., Yang, T., Lin, Y. and Johnson, J. (2009) Effects of palmitate on ER and cytosolic Ca^{2+} homeostasis in beta-cells. *Am. J. Physiol. Endocrinol. Metab.*, **296**, E690–E701.
5. Tessitore, A., del P Martin, M., Sano, R., Ma, Y., Mann, L., Ingrassia, A., Laywell, E., Steindler, D., Hendershot, L. and d'Azzo, A. (2004) GM1-ganglioside-mediated activation of the unfolded protein response causes neuronal death in a neurodegenerative gangliosidosis. *Mol. Cell*, **15**, 753–766.
6. Pelled, D., Trajkovic-Bodennec, S., Lloyd-Evans, E., Sidransky, E., Schiffmann, R. and Futerman, A. (2005) Enhanced calcium release in the acute neuronopathic form of Gaucher disease. *Neurobiol. Dis.*, **18**, 83–88.
7. Hara, T., Mahadevan, J., Kanekura, K., Hara, M., Lu, S. and Urano, F. (2014) Calcium efflux from the endoplasmic reticulum leads to β-cell death. *Endocrinology*, **155**, 758–768.
8. Pozzan, T., Rizzuto, R., Volpe, P. and Meldolesi, J. (1994) Molecular and cellular physiology of intracellular calcium stores. *Physiol. Rev.*, **74**, 595–636.
9. Sano, R., Annunziata, I., Patterson, A., Moshiach, S., Gomero, E., Opferman, J., Forte, M. and d'Azzo, A. (2009) GM1-ganglioside accumulation at the mitochondria-associated ER membranes links ER stress to Ca(2+)-dependent mitochondrial apoptosis. *Mol. Cell*, **36**, 500–511.
10. Pelled, D., Lloyd-Evans, E., Riebeling, C., Jeyakumar, M., Platt, F. and Futerman, A. (2003) Inhibition of calcium uptake via the sarco/endoplasmic reticulum Ca2+-ATPase in a mouse model of Sandhoff disease and prevention by treatment with *N*-butyldeoxynojirimycin. *J. Biol. Chem.*, **278**, 29496–29501.
11. Thuerauf, J., Hoover, H., Meller, J., Hernandez, J., Su, L., Andrews, C., Dillmann, W., McDonough, P. and Glembotski, C. (2001) Sarco/endoplasmic reticulum calcium ATPase-2 expression is regulated by ATF6 during the endoplasmic reticulum stress response: intracellular signalling of calcium stress in cardiac myocytes model system. *J. Biol. Chem.*, **276**, 48309–48317.
12. Barrett, T., Bundey, S. and Macleod, A. (1995) Neurodegeneration and diabetes-UK nationwide study of Wolfram (DIDMOAD) syndrome. *Lancet*, **346**, 1458–1463.
13. Inoue, H., Tanizawa, Y., Wasson, J., Behn, P., Kalidas, K., Bernal-Mizrachi, E., Mueckler, M., Marshall, H., Donis-Keller, H., Crock, P. *et al.* (1998) A gene encoding a transmembrane protein is mutated in patients with diabetes mellitus and optic atrophy (Wolfram syndrome). *Nat. Genet.*, **20**, 143–148.
14. Fonseca, S., Fukuma, M., Lipson, K., Nguyen, L., Allen, J., Oka, Y. and Urano, F. (2005) WFS1 is a novel component of the unfolded protein

response and maintains homeostasis of the endoplasmic reticulum in pancreatic beta cells. *J. Biol. Chem.*, **280**, 39609–39615.
15. Fonseca, S.G., Ishigaki, S., Oslowski, C., Lu, S., Lipson, K., Ghosh, R., Hayashi, E., Ishihara, H., Oka, Y., Permutt, M. and Urano, F. (2010) Wolfram syndrome 1 gene negatively regulates ER stress signalling in rodent and human cells. *J. Clin. Invest.*, **120**, 744–755.
16. Riggs, A., Bernal-Mizrachi, E., Ohsugi, M., Wasson, J., Fatrai, S., Welling, C., Murray, J., Schmidt, R., Herrera, P. and Permutt, M. (2005) Mice conditionally lacking the Wolfram gene in pancreatic islet beta cells exhibit diabetes as a result of enhanced endoplasmic reticulum stress and apoptosis. *Diabetologia*, **48**, 2313–2321.
17. Isihara, H., Takeda, S., Tamura, A., Takahashi, R., Yamaguchi, S., Takei, D., Yamada, T., Inoue, H., Soga, H., Katagiri, H., Tanizawa, Y. and Oka, Y. (2004) Disruption of the WFS1 gene in mice causes progressive beta cell loss and impaired stimulus-secretion coupling in insulin secretion. *Hum. Mol. Genet.*, **13**, 1159–1170.
18. Takei, D., Ishihara, H., Yamaguchi, S., Yamada, T., Tamura, A., Katagiri, H., Maruyama, Y. and Oka, Y. (2006) WFS1 protein modulates the free Ca(2+) concentration in the endoplasmic reticulum. *FEBS Lett.*, **580**, 5635–5640.
19. Osman, A., Saito, M., Makepeace, C., Permutt, M., Schlesinger, P. and Mueckler, M. (2003) Wolframin expression induces novel ion channel activity in endoplasmic reticulum membranes and increases intracellular calcium. *J. Biol. Chem.*, **278**, 52755–52762.
20. Zatyka, M., Ricketts, C., da Silva Xavier, G., Minton, J., Fenton, S., Hofmann-Thiel, S., Rutter, G.A. and Barrett, T.G. (2008) Sodium potassium ATPase beta 1 subunit is a molecular partner of Wolframin, an endoplasmic reticulum protein involved in ER stress. *Hum. Mol. Genet.*, **17**, 190–200.
21. Gharanei, S., Zatyka, M., Astuti, D., Fenton, J., Sik, A., Nagy, Z. and Barrett, T.G. (2013) Vacuolar-type H+ ATPase V1A subunit is a molecular partner of Wolfram syndrome 1 (WFS1) protein, which regulates its expression and stability. *Hum. Mol. Genet.*, **22**, 203–217.
22. Fonseca, S., Urano, F., Weir, G., Gromada, J. and Burcin, M. (2012) Wolfram syndrome 1 and adenylyl cyclase 8 interact at the plasma membrane to regulate insulin production and secretion. *Nat. Cell Biol.*, **14**, 1105–1112.
23. Ainscow, E.K. and Rutter, G.A. (2001) Mitochondrial priming modifies Ca^{2+} oscillations and insulin secretion in pancreatic islets. *Biochem. J.*, **353**, 175–180.
24. Kennedy, H.J., Pouli, A.E., Ainscow, E.K., Jouaville, L.S., Rizzuto, R. and Rutter, G.A. (1999) Glucose generates sub-plasma membrane ATP microdomains in single islet beta cells. Potential role for strategically located mitochondria. *J. Biol. Chem.*, **274**, 13281–13291.
25. Jouaville, L.S., Pinton, P., Bastianutto, C., Rutter, G.A. and Rizzuto, R. (1999) Regulation of mitochondrial ATP synthesis by calcium: evidence for long term metabolic priming. *Proc. Natl. Acad. Sci. USA*, **96**, 13807–13812.
26. Bell, C.J., Manfredi, G., Griffiths, E.J. and Rutter, G.A. (2007) Luciferase expression for ATP imaging: application to cardiac myocytes. *Methods Cell Biol.*, **80**, 341–352.
27. Ainscow, E.K., Zhao, C. and Rutter, G.A. (2000) Acute overexpression of lactate dehydrogenase-A perturbs beta cell mitochondrial metabolism and insulin secretion. *Diabetes*, **49**, 1149–1155.
28. Ainscow, E.K. and Rutter, G.A. (2002) Glucose-stimulated oscillations in free cytosolic ATP concentration imaged in single islet beta-cells: evidence for a Ca^{2+} dependent mechanism. *Diabetes*, **51** (Suppl 1), S162–S170.
29. Owen, M.R. (1993) The mechanisms by which mild respiratory chain inhibitors regulate hepatic gluconeogenesis. PhD thesis. University of Bristol.
30. Barrett, T.G., Poulton, K. and Bundey, S. (1995) DIDMOAD syndrome; further studies and muscle biopsy. *J. Inherit. Metab. Dis.*, **18**, 218–220.
31. Lai, P. and Michelangeli, F. (2009) Changes in expression and activity of the secretory pathway Ca^{2+}ATPase1 (SPCA1) in A7r5 vascular smooth muscle cells cultured at different glucose concentration. *Biosci. Rep.*, **29**, 397–404.
32. Sayers, L.G., Brown, G.R., Michell, R.H. and Michelangeli, F. (1993) The effects of thimerosal on calcium uptake and inositol 1,4,5-trisphosphate-induced calcium release in cerebellar microsomes. *Biochem. J.*, **289**, 883–887.
33. Bergsten, P., Grapengiesser, E., Gylfe, E., Tengholm, A. and Hellman, B. (1994) Synchronous oscillations of cytoplasmic Ca^{2+} and insulin release in glucose stimulated pancreatic islets. *J. Biol. Chem.*, **269**, 8749–8753.
34. Longo, E.A., Tornheim, K., Deeney, J.T., Varnum, B.A., Tillotson, D., Prentki, M. and Corkey, B.E. (1991) Oscillations in cytosolic free Ca^{2+}, oxygen consumption and insulin secretion in glucose stimulated rat pancreatic islets. *J. Biol. Chem.*, **266**, 9314–9319.
35. Kravtsova-Ivantsiv, Y. and Ciechanover, A. (2012) Non-canonical ubiquitin-based signals for proteasomal degradation. *J. Cell Sci.*, **125**, 539–548.
36. Kuo, T.H., Liu, B.F., Yu, Y., Wuytack, F., Raeymaekers, L. and Tsang, W. (1997) Coordinated regulation of the plasma membrane calcium pump and the sarco(endo)plasmic reticular calcium pump gene expression by Ca2+. *Cell Calcium*, **21**, 399–408.
37. Caspersen, C., Pedersen, P.S. and Treiman, M. (2000) The sarco/endoplasmic reticulum calcium-ATPase 2b is an endoplasmic reticulum stress-inducible protein. *J. Biol. Chem.*, **275**, 22363–22372.
38. Hojmann Larsen, A., Frandsen, A. and Treiman, M. (2001) Upregulation of the SERCA type Ca^{2+} pump activity in response to endoplasmic reticulum stress in PC12 cells. *BMC Biochem.*, **2**, 4.
39. Fredersdorf, S., Thumann, C., Zimmermann, W.H., Vetter, R., Graf, T., Luchner, A., Riegger, G.A., Schunkert, H., Eschenhagen, T. and Weil, J. (2012) Increased myocardial SERCA expression in early type 2 diabetes mellitus is insulin dependent: in vivo and in vitro data. *Cardiovasc. Diabetol.*, **11**, 57.
40. Wu, K-D., Bungard, D. and Lytton, J. (2001) Regulation of SERCA Ca^{2+} pump expression by cytoplasmic [Ca^{2+}] in vascular smooth muscle cells. *Am. J. Physiol. Cell Physiol.*, **280**, C843–C851.
41. Cordozo, A.K., Ortis, F., Storling, J., Feng, Y.M., Rasschaert, J., Tonnesen, M., Van Eylen, F., Mandrup-Poulsen, T., Herchueltz, A. and Eizirik, D.L. (2005) Cytokines downregulate the sarcoendoplasmic reticulum pump Ca^{2+}ATPase 2b and deplete endoplasmic reticulum Ca^{2+}, leading to induction of endoplasmic reticulum stress in pancreatic β-cells. *Diabetes*, **54**, 452–461.
42. Park, S.W., Zhou, Y., Lee, J., Lee, J. and Ozcan, U. (2010) Sarco(endo)plasmic reticulum Ca^{2+} ATPase 2b is a major regulator of endoplasmic reticulum stress and glucose homeostasis in obesity. *Proc. Natl. Acad. Sci. USA*, **107**, 19320–19325.
43. Mitchell, K.J., Tsuboi, T. and Rutter, G.A. (2004) Role for plasma membrane-related Ca2+ATPase-1 (ATP2C1) in pancreatic beta-cell Ca^{2+} homeostasis revealed by RNA silencing. *Diabetes*, **53**, 393–400.
44. da Silva Xavier, G., Mondragon, A., Sun, G., Chen, L., Mc Ginty, J.A., French, P.M. and Rutter, G.A. (2012) Abnormal glucose tolerance and insulin secretion in pancreas specific Tcf712-null mice. *Diabetologia*, **55**, 2667–2676.
45. Montero, M., Brini, M., Marsault, R., Alvarez, J., Sitia, R., Pozzan, T. and Rizzuto, R. (1995) Monitoring dynamic changes in free Ca^{2+} concentration in the endoplasmic reticulum of intact cells. *EMBO J.*, **14**, 5467–5475.
46. Mitchell, K.J., Pinton, P., Varadi, A., Tacchetti, C., Ainscow, E.K., Pozzan, T., Rizzuto, R. and Rutter, G.A. (2001) Dense core secretory vesicles revealed as a dynamic Ca(2+) store in neuroendocrine cells with a vesicle-associated membrane protein aequorin chimaera. *J. Cell Biol.*, **155**, 41–51.
47. Brini, M., Marsault, R., Bastianutto, C., Alvarez, J., Pozzan, T. and Rizzuto, R. (1995) Transfected aequorin in the measurement of cytosolic Ca^{2+} concentration ([Ca^{2+}]c): a critical evaluation. *J. Biol. Chem.*, **270**, 9896–9903.
48. Varadi, A., Cirulli, V. and Rutter, G.A. (2004) Mitochondrial localization as a determinant of capacitative Ca2+ entry in HeLa cells. *Cell Calcium*, **36**, 499–508.
49. Cobbold, P. and Rink, T. (1987) Fluorescence and luminescence measurement of cytoplasmic free calcium. *Biochem. J.*, **248**, 313–328.
50. Rutter, G.A., Theler, J., Murgia, M., Wollheim, C.B., Pozzan, T. and Rizzuto, R. (1993) Stimulated Ca^{2+} influx rises mitochondrial free Ca^{2+} to supramicromolar levels in a pancreatic beta cell line. Possible role in glucose and agonist induced insulin secretion. *J. Biol. Chem.*, **268**, 22385–22390.
51. Alvarez, J. and Montero, M. (2002) Measuring [Ca^{2+}] in the endoplasmic reticulum with aequorin. *Cell Calcium*, **32**, 251–260.